

Supporting Information

Dual mimic enzyme properties of Fe nanoparticles embedded in two-dimensional carbon nanosheets for colorimetric detection of biomolecules

Jie Wang,^{‡a} Chenglong Zhao,^{‡a} Feijin Zhou,^a Hui Lu,^b Zhenhong Huang,^b Cheng
Yao^{*a} and Chan Song^{*a}

^a *School of Chemistry and Molecular Engineering, Nanjing Tech University, Nanjing
211816, China; Email: yaocheng@njtech.edu.cn; songchan@njtech.edu.cn*

^b *Jiangsu Zhongdan Group Co., Ltd., Taixing 225453, China*

[‡] These two authors contributed equally to this work.

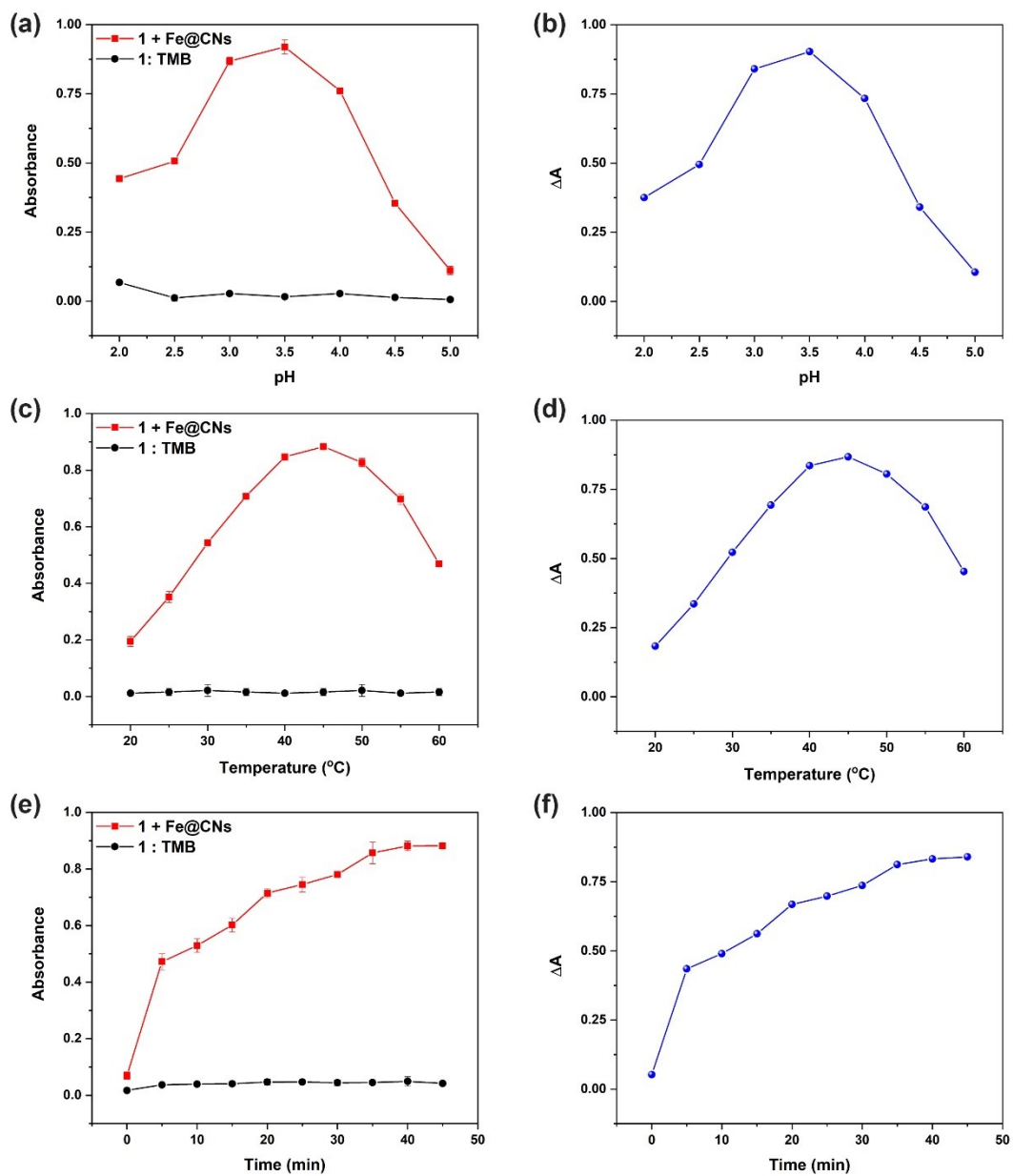


Fig. S1 The effect of pH (a, b), reaction temperature (c, d), and incubation time (e, f) on the oxidase-like activity of Fe@CNs (0.2 g L^{-1}). ΔA is the enhancement of absorbance intensity at 652 nm of the catalytic system ($A - A_0$). A and A_0 are the absorbance intensity at 652 nm of TMB (0.2 mM .) with and without Fe@CNs, respectively.

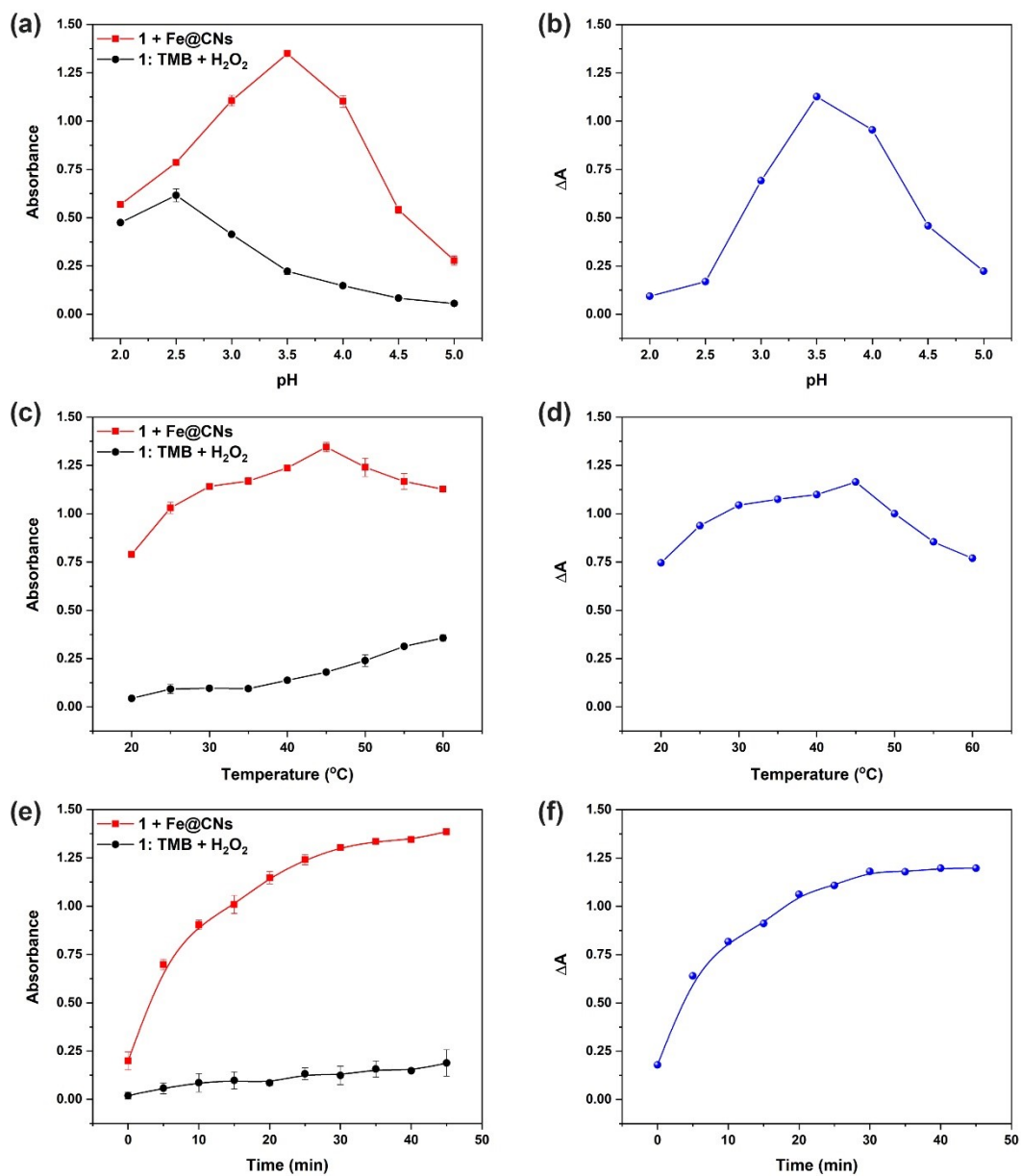


Fig. S2 The effect of pH (a, b), reaction temperature (c, d), and incubation time (e, f) on the peroxidase-like activity of Fe@CNs (0.2 g L^{-1}). ΔA is the enhancement of absorbance intensity at 652 nm of the catalytic system ($A - A_0$). A and A_0 are the absorbance intensity at 652 nm of TMB (0.2 mM) and H_2O_2 (0.1 mM) with and without Fe@CNs, respectively.

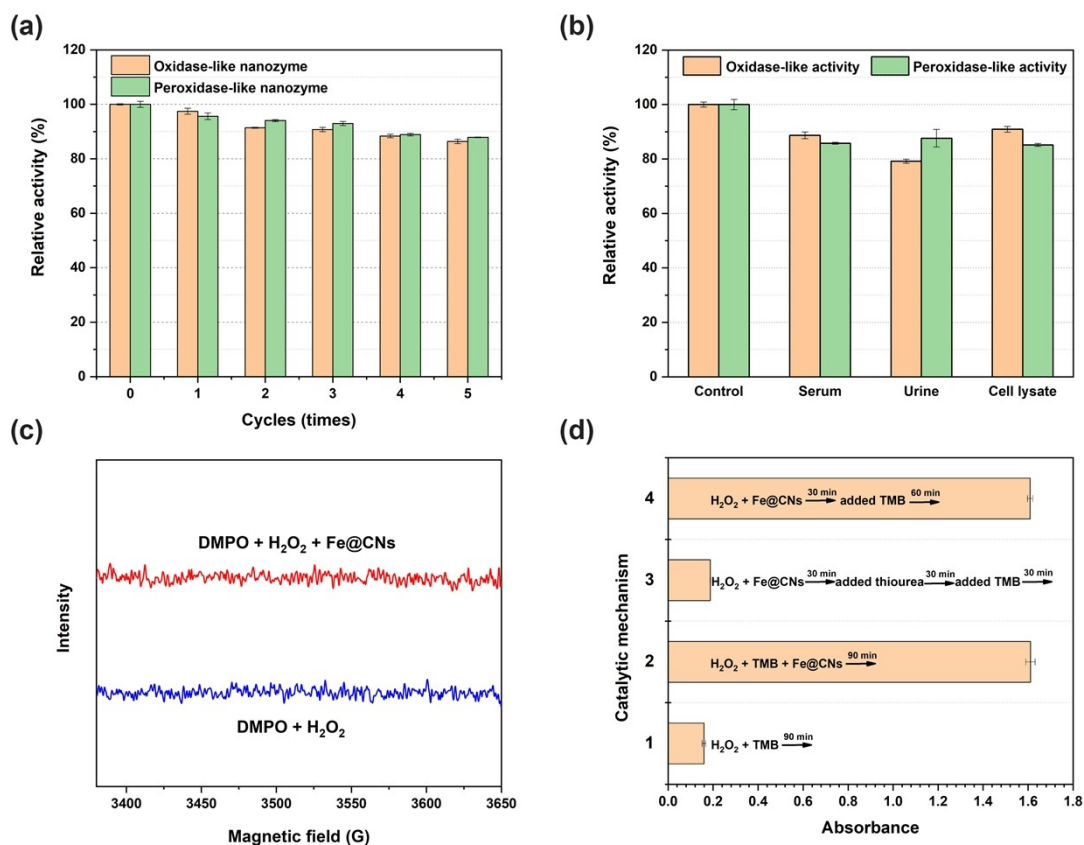


Fig. S3 (a) The reusability of Fe@CNs as the oxidase-like nanozyme and peroxidase-like nanozyme in the catalytic system. (b) The catalytic activity of Fe@CNs in the catalytic system with the presence of 1% serum sample, 1% urine sample, and 1% cell lysate, respectively. (c) DMPO (100 mM) and H₂O₂ (100 mM) with and without Fe@CNs (50 mg L⁻¹) by using methanol as solvent. The sample was conducted in the condition without oxygen. (d) The absorbance intensity at 652 nm of the samples without oxygen under different experimental condition. Inset: schematic representations of the different reaction routes and ingredients. The total volume of samples was 1.5 mL.

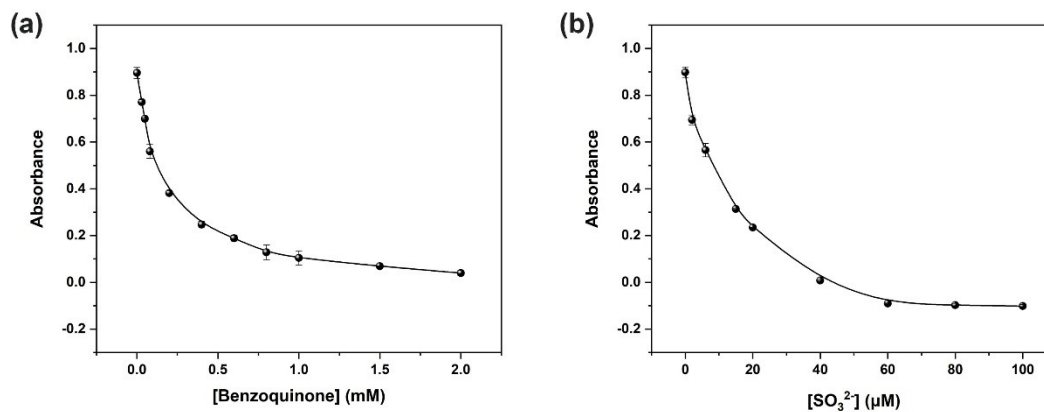


Fig. S4 The effect of benzoquinone (a) and SO_3^{2-} (b) on the oxidase-like activity of Fe@CNs.

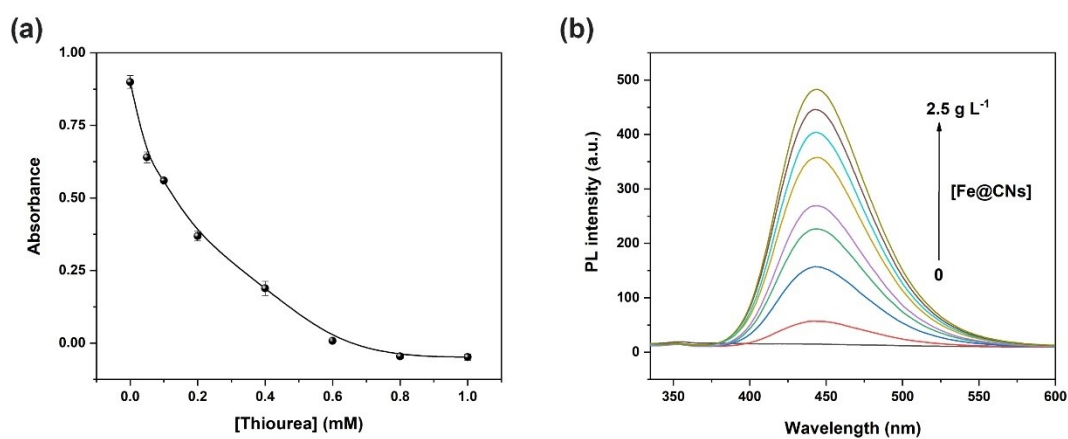


Fig. S5 (a) The effect of thiourea with different concentration (0, 0.05, 0.1, 0.2, 0.4, 0.6, 0.8 and 1.0 mM) on the peroxidase-like activity of Fe@CNs. $[\text{Fe@CNs}] = 0.2 \text{ g L}^{-1}$, $[\text{TMB}] = 0.2 \text{ mM}$, $[\text{H}_2\text{O}_2] = 0.1 \text{ mM}$. (b) Phosphorescent intensity of the sample containing TA (0.625 mM), H_2O_2 (50 mM) and different concentration of Fe@CNs (0, 0.1, 0.25, 0.4, 0.5, 1.0, 1.5, 2.0 and 2.5 g L^{-1}) under pH 3.5 with an excitation wavelength of 314 nm.

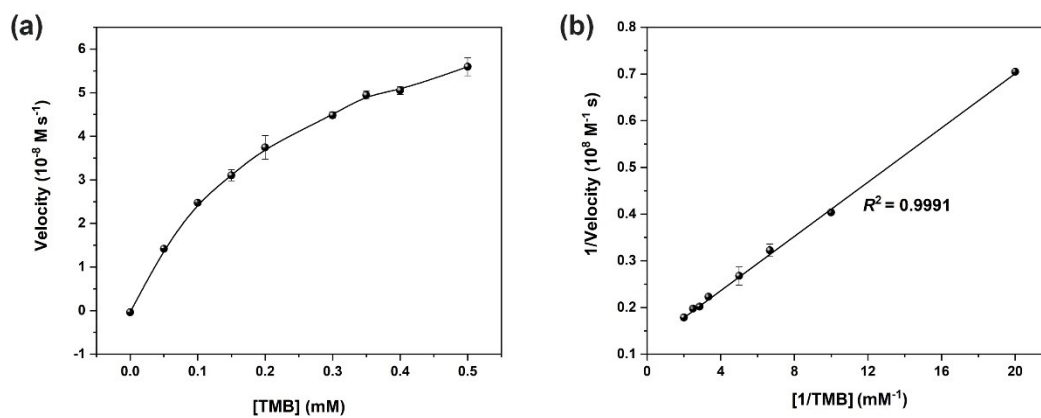


Fig. S6 Steady-state kinetic analysis by using the Michaelis-Menten model (a) and Lineweaver-Burk double-reciprocal model (b) for the oxidase-like activity of Fe@CNs (0.2 g L^{-1}) at pH 3.5.

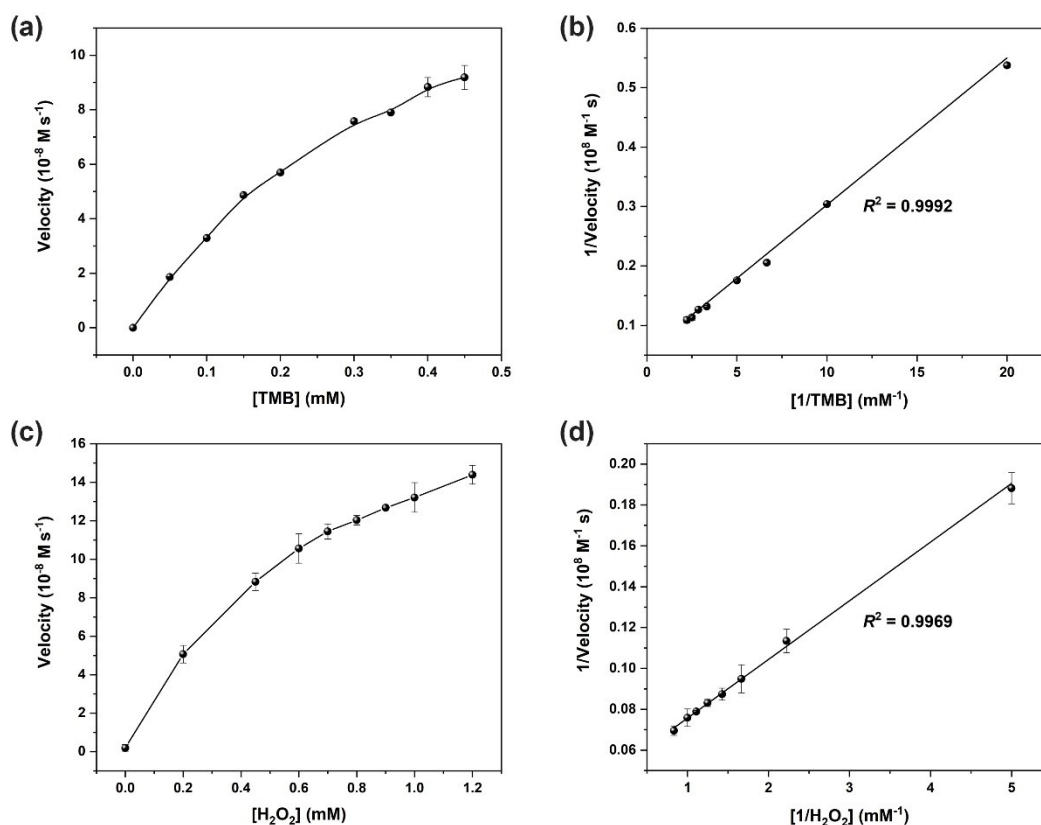


Fig. S7 Steady-state kinetic analysis by using the Michaelis-Menten model (a and c) and Lineweaver-Burk double-reciprocal model (b and d) for the peroxidase-like activity of Fe@CNs (0.2 g L⁻¹) at pH 3.5. (a) Reaction velocity plot with a fixed H₂O₂ concentration (0.1 mM) and various TMB amount. (c) Reaction velocity plot with a fixed TMB concentration (0.2 mM) and various H₂O₂ amount. (b) and (d) Double reciprocal plots for Fe@CNs with the amount of one substrate (TMB or H₂O₂) varied.

Table S1. The Michaelis-Menten constant (K_m) of Fe@CNs and other nanomaterial-based oxidase-like nanozymes to TMB.

Catalyst	K_m (mM)	Reference
PCN-222 (Fe)	1.63	1
Fe-Co-LDH	0.34	2
Fe(III)-L3	2.03	3
CS/Cu/Fe composite	0.27	4
Dex-FeMnzyme	0.33	5
Fe@CNs	0.24	this work

Table S2. The Michaelis-Menten constant (K_m) and maximum reaction velocity (V_{max}) of HRP, Fe@CNs and other nanomaterial-based peroxidase-like nanozymes to H_2O_2 and TMB.

Catalysts	Substrate	K_m (mM)	V_m (10^{-8} M s $^{-1}$)	Reference
HRP	H_2O_2	3.70	8.71	6
	TMB	0.43	10.00	
ZnFe $_2$ O $_4$ MNPs	H_2O_2	1.66	7.74	7
	TMB	0.85	13.31	
Fe-NDs	H_2O_2	0.87	3.76	8
	TMB	0.76	2.27	
Fe-MOF	H_2O_2	1.3	2.5	9
	TMB	2.6	5.6	
Fe@CNs	H_2O_2	0.50	21.22	this work
	TMB	0.45	18.07	

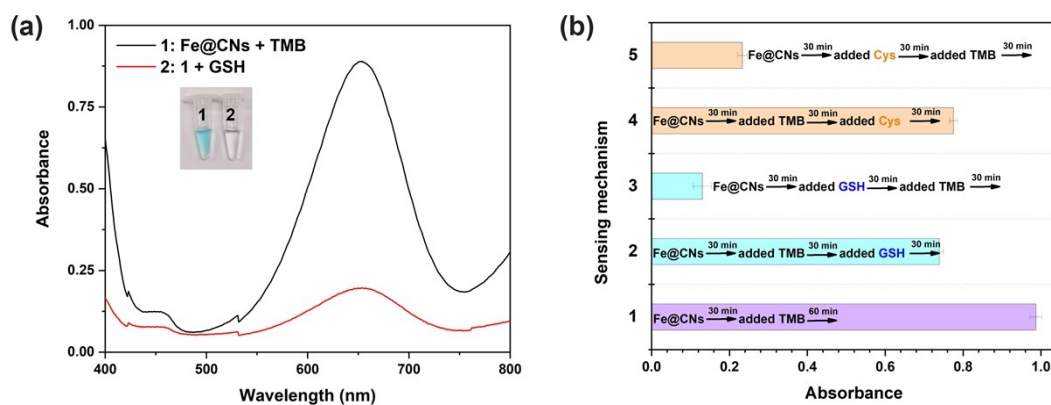


Fig. S8 (a) UV-vis absorption curves of Fe@CNs (0.2 g L^{-1}) and TMB (0.2 mM) without and with GSH ($100 \text{ }\mu\text{M}$), respectively. (b) The GSH/Cys sensing mechanism based on the oxidase-like catalytic activity of Fe@CNs. Inset: schematic representations of the different reaction routes and ingredients.

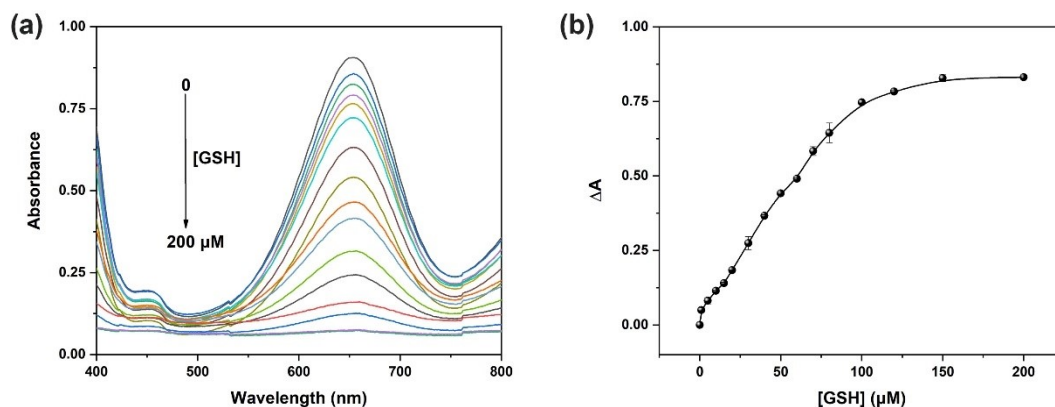


Fig. S9 (a) UV-vis absorption curves of Fe@CNs (0.2 g L^{-1}) with TMB (0.2 mM) and different amounts of GSH. (b) The absorbance changes with increasing concentration of GSH. ΔA is the enhancement of absorbance intensity at 652 nm of the catalytic system ($A_0 - A$). A_0 and A are the absorbance intensity at 652 nm of Fe@CNs and TMB without and with GSH, respectively.

Table S3. Comparison of different nanomaterial-based nanozymes as the sensing platform for GSH detection by colorimetric method.

Nanozyme	Linear range (μM)	Detection limit (μM)	Reference
$\text{Cu}_{1.8}\text{S}$ NPs	500-10000	60	10
CuS-PDA-Au	0.5-100	0.42	11
CBT-Cys(SEt)	0-87	1	12
Au NCs	2-25	0.42	13
Por-ZnFe ₂ O ₄ /rGO	2-40	0.76	14
Fe ₃ O ₄ NPs	3-30	3.0	15
MnO ₂ NSs	1-25	0.3	16
PS MOF	0-20	0.68	17
Fe@CNs	1-80	0.22	this work

Table S4. Recoveries of GSH, H₂O₂ and glucose in 1% human serum sample.

Target	Added (μM)	Recovered (μM)			Recovery (%)
GSH	20	19.0	19.9	21.3	100.55 \pm 5.79
	40	36.5	41.4	40.9	98.96 \pm 6.66
	60	65.6	58.3	65.2	105.09 \pm 6.82
H ₂ O ₂	50	51.8	47.3	48.2	98.22 \pm 4.75
	100	100.1	102.0	102.3	101.48 \pm 1.17
	150	157.5	165.3	152.3	105.51 \pm 4.45
glucose	50	49.9	46.6	50.8	98.22 \pm 4.47
	100	107.6	101.7	95.0	101.43 \pm 6.27
	150	155.1	151.6	158.6	103.40 \pm 2.36

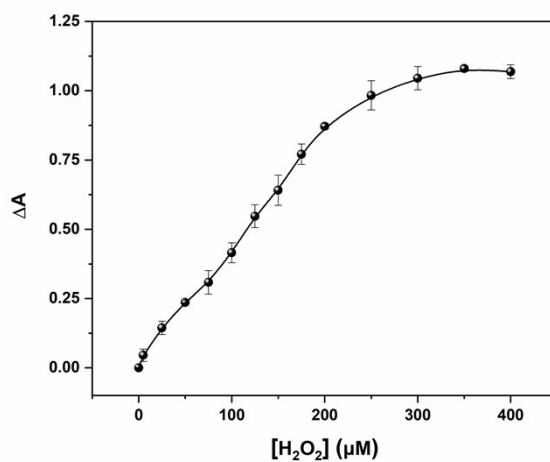


Fig. S10 The absorbance changes with increasing concentration of H₂O₂. ΔA is the enhancement of absorbance intensity at 652 nm of the catalytic system ($A-A_0$). A and A_0 are the absorbance intensity at 652 nm of Fe@CNs (0.2 g L⁻¹) and TMB (0.2 mM) with and without H₂O₂, respectively.

Table S5. Comparison of different nanomaterial-based peroxidase-like nanozyme as the sensing platform for H₂O₂ detection by colorimetric method.

Nanozyme	Linear range (μM)	Detection limit (μM)	Reference
Cys-MoS ₂ NFs	0-300	4.103	18
CePO ₄ -CeO ₂	5-150	2.9	19
FeMnO ₃ @PPy NTs	0-100	3.2	20
FePPOP-1	20-1000	6.5	21
CuZnFeS NCs	10-55	3	22
M-CQDs	20-200	15	23
ZIF-67	1×10^5 - 1×10^6	110	24
CDs@ZIF-8-a	100-1000	3.6	25
Fe@CNs	5-200	2.04	this work

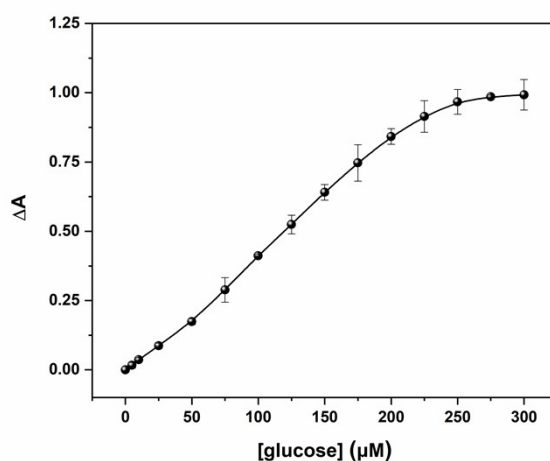


Fig. S11 The absorbance changes with increasing concentration of glucose. ΔA is the enhancement of absorbance intensity at 652 nm of the catalytic system ($A - A_0$). A and A_0 are the absorbance intensity at 652 nm of Fe@CNs (0.2 g L^{-1}) and TMB (0.2 mM) with and without glucose, respectively.



Fig. S12 The photographs of the specificity analysis of the glucose detection. The concentration of the interfering species, and glucose was $150 \mu\text{M}$.

Table S6. Comparison of different nanomaterial-based peroxidase-like nanozyme as the sensing platform for glucose detection by colorimetric method.

Nanozyme	Linear range (μM)	Detection limit (μM)	Reference
FePPOPs-SO ₃ H	200-1500	16.38	26
CeO ₂ /Zeolite Y	0-340	35.4	27
Fe ₃ O ₄ MNPs	50-1000	30	28
6Fe/CeO ₂ NRs	1-100	3.41	29
Fe@PCN-224 NPs	30-800	22	30
WSe ₂ NSs	10-60	10	31
CoPW ₁₁ O ₃₉	33-500	23.4	32
Co ₃ O ₄ NPs	20-200	5	33
Fe@CNs	5-225	2.28	this work

Reference

1. D. Feng, Z. Y. Gu, J. R. Li, H. L. Jiang, Z. Wei and P. D. H.-C. Zhou, *Angew. Chem.* 2012, 51, 10307-10310.
2. X. Xu, X. Zou, S. Wu, L. Wang, J. Pan, M. Xu, W. Shan, X. Li and X. Niu, *Microchim Acta.* 2019, 186, 815.
3. L. Zhang, Y. Hou, X. Guo, W. Liu, C. Lv, C. Zhang, Y. Jin and B. Li, *Luminescence.* 2020, 35, 1350-1359.
4. Y. Zou, Q. Chai, T. Zhu, X. Yu, G. Mao, N. Li, J. Chen and G. Lai, *Spectrochim. Acta A Mol. Biomol.* 2022, 266, 120410.
5. X. Han, L. Liu, H. Gong, L. Luo, Y. Han, J. Fan, C. Xu, T. Yue, J. Wang and W. Zhang, *Food Chem.* 2022, 371, 131115.
6. Y. Guo, L. Deng, J. Li, S. Guo, E. Wang and S. Dong, *ACS Nano.* 2011, 5, 1282-1290.
7. L. Su, J. Feng, X. Zhou, C. Ren, H. Li and X. Chen, *Anal. Chem.* 2012, 84, 5753-5758.
8. Y. Liu, J. Yan, Y. Huang, Z. Sun, H. Zhang, L. Fu, X. Li and Y. Jin, *Front. Bioeng. Biotechnol.* 2022, 9, 790849.
9. W. Xu, L. Jiao, H. Yan, Y. Wu, L. Chen, W. Gu, D. Du, Y. Lin and C. Zhu, *ACS Appl Mater Inter.* 2019, 11, 22096-22101.
10. H. Zou, T. Yang, J. Lan and C. Huang, *Anal. Methods.* 2017, 9, 841-846.
11. Y. Wang, Y. Liu, F. Ding, X. Zhu, L. Yang, P. Zou, H. Rao, Q. Zhao and X. Wang, *Anal Bioanal Chem.* 2018, 410, 4805-4813.
12. Y. Yuan, J. Zhang, M. Wang, B. Mei, Y. Guan and G. Liang, *Anal. Chem.* 2013, 85, 1280-1284.
13. J. Feng, P. Huang, S. Shi, K.-Y. Deng and F.-Y. Wu, *Anal. Chim. Acta.* 2017, 967, 64-69.
14. B. Bian, Q. Liu and S. Yu, *Colloids Surf. B.* 2019, 181, 567-575.
15. Y. Ma, Z. Zhang, C. Ren, G. Liu and X. Chen, *Analyst.* 2012, 137, 485-489.
16. J. Liu, L. Meng, Z. Fei, P. J. Dyson, X. Jing and X. Liu, *Biosens. Bioelectron.* 2017, 90, 69-74.
17. Y. Liu, M. Zhou, W. Cao, X. Wang, Q. Wang, S. Li and H. Wei, *Anal. Chem.* 2019, 91, 8170-8175.
18. J. Yu, D. Ma, L. Mei, Q. Gao, W. Yin, X. Zhang, L. Yan, Z. Gu, X. Ma and Y. Zhao, *J Mater Chem B.* 2018, 6, 487-498.
19. G. Vinothkumar, A. I. Lalitha and K. Suresh Babu, *Inorg. Chem.* 2018, 58, 349-358.
20. M. Chi, S. Chen, M. Zhong, C. Wang and X. Lu, *Chem. Comm.* 2018, 54, 5827-5830.
21. C. Cui, Q. Wang, Q. Liu, X. Deng, T. Liu, D. Li and X. Zhang, *Sens. Actuators B Chem.* 2018, 277, 86-94.
22. A. Dalui, B. Pradhan, U. Thupakula, A. H. Khan, G. S. Kumar, T. Ghosh, B. Satpati and S. Acharya, *Nanoscale,* 2015, 7, 9062-9074.
23. S. Chandra, V. K. Singh, P. K. Yadav, D. Bano, V. Kumar, V. K. Pandey, M. Talat and S. H. Hasan, *Anal. Chim. Acta.* 2019, 1054, 145-156.
24. S. Wang, D. Xu, L. Ma, J. Qiu, X. Wang, Q. Dong, Q. Zhang, J. Pan and Q. Liu, *Anal. Bioanal. Chem.* 2018, 410, 7145-7152.
25. Y. Wang, X. Liu, M. Wang, X. Wang, W. Ma and J. Li, *Sens. Actuators B Chem.* 2021, 329, 129115.
26. T. Liu, J. Tian, L. Cui, Q. Liu, L. Wu and X. Zhang, *Colloids Surf. B.* 2019, 178, 137-145.
27. X. Cheng, L. Huang, X. Yang, A. A. Elzatahry, A. Alghamdi and Y. Deng, *J. Colloid*

- Interface Sci.* 2019, 535, 425-435.
28. H. Wei and E. Wang, *Anal. Chem.* 2008, 80, 2250-2254.
29. Jampaiah. D, Srinivasa Reddy. T, Kandjani. A. E, Selvakannan. P. R, Sabri. Y. M, Coyle. V. E, Shukla. R and Bhargava. S. K, *J Mater Chem B.* 2016, 4, 3874-3885.
30. T. Li, P. Hu, J. Li, P. Huang, W. Tong and C. Gao, *Colloids Surf. A Physicochem. Eng. Asp.* 2019, 577, 456-463.
31. T. Chen, X. Wu, J. Wang and G. Yang, *Nanoscale.* 2017, 9, 11806-11813.
32. Y. He, X. Li, X. Xu, J. Pan and X. Niu, *J Mater Chem B.* 2018, 6, 5750-5755.
33. H. Jia, D. Yang, X. Han, J. Cai, H. Liu and W. He, *Nanoscale.* 2016, 8, 5938-5945.